Acta Crystallographica Section E
**Structure Reports Online**
ISSN 1600-5368

# Redetermination of the low-temperature polymorph of $Li_2MnSiO_4$ from single-crystal X-ray data

**Mineo Sato,[a]* Tadashi Ishigaki,[b] Kazuyoshi Uematsu,[a] Kenji Toda[c] and Hirokazu Okawa[d]**

[a]Department of Chemistry and Chemical Engineering, Faculty of Engineering, Niigata University, Ikarashi 2-no-cho, Niigata City 950-2181, Japan, [b]Center for Transdiciplinary Research, Niigata University, 8050 Ikarashi 2-no-cho, Niigata 950-2181, Japan, [c]Graduate School of Science and Technology, Niigata University, 8050 Ikarashi 2-nocho, Niigata 950-2181, Japan, and [d]Department of Earth Science and Technology, Faculty of Engineering and Resource Science, Akita University, Tegata Gakuen-machi, Akita 010-8502, Japan
Correspondence e-mail: msato@eng.niigata-u.ac.jp

Received 5 July 2012; accepted 8 August 2012

Key indicators: single-crystal X-ray study; $T$ = 295 K; mean $\sigma$(Si–O) = 0.002 Å; $R$ factor = 0.015; $wR$ factor = 0.037; data-to-parameter ratio = 9.4.

Crystals of dilithium manganese(II) silicate were grown under high-temperature hydrothermal conditions in the system $LiOH-MnO_2-SiO_2$. The title compound crystallizes in the $\beta_{II}$-$Li_3PO_4$ structure type. The coordination polyhedra of all cations are slightly distorted tetrahedra ($m$ symmetry for $MnO_4$ and $SiO_4$), which are linked by corner-sharing to each other. The vertices of the tetrahedra point to the same direction perpendicular to the distorted hexagonal close-packed (hcp) array of O atoms within which half of the tetrahedral voids are occupied by cations. In comparison with the previous refinement from powder X-ray data [Dominko *et al.* (2006). *Electrochem. Commun.* **8**, 217–222], the present reinvestigation from single-crystal X-ray data allows a more precise determination of the distribution of the $Li^+$ and $Mn^{2+}$ cations, giving a perfectly site-ordered structure model for both $Li^+$ and $Mn^{2+}$.

## Related literature

For background to structural studies of $Li_2MSiO_4$ ($M$ = Mn, Fe, Co) compounds, see: Islam *et al.* (2011); Santamaría-Pérez *et al.* (2012); Setoguchi (1988); Yamaguchi *et al.* (1979). Polymorphism of $Li_2MnSiO_4$ was reported by Arroyo-de Dompablo *et al.* (2006, 2008); Belharouak *et al.* (2009); Dominko *et al.* (2006); Kokalj *et al.* (2007); Politaev *et al.* (2007); Wu *et al.* (2009); Zhong *et al.* (2010). For notation of $Li_3PO_4$ polymorphs, see: West & Glasser (1972). For theoretical studies of the redox potentials and Li migration paths of $Li_2MnSiO_4$, see: Kuganathan & Islam (2009); Mali *et al.* (2010); Duncan *et al.* (2011), and for NMR studies of this material, see: Sirisopanaporn *et al.* (2011). For the bond-valence method, see: Brown & Altermatt (1985). For crystallographic background, see: Cooper *et al.* (2002).

## Experimental

### Crystal data

$Li_2MnSiO_4$
$M_r$ = 160.91
Orthorhombic, $Pmn2_1$
$a$ = 6.3133 (16) Å
$b$ = 5.3677 (14) Å
$c$ = 4.9685 (12) Å
$V$ = 168.37 (7) Å$^3$
$Z$ = 2
Mo $K\alpha$ radiation
$\mu$ = 4.11 mm$^{-1}$
$T$ = 295 K
0.26 × 0.19 × 0.18 mm

### Data collection

Rigaku Mercury375R diffractometer
Absorption correction: multi-scan (*REQAB*; Rigaku, 1998)
$T_{min}$ = 0.377, $T_{max}$ = 0.477
1636 measured reflections
423 independent reflections
419 reflections with $I > 2\sigma(I)$
$R_{int}$ = 0.019

### Refinement

$R[F^2 > 2\sigma(F^2)]$ = 0.015
$wR(F^2)$ = 0.037
$S$ = 1.14
423 reflections
45 parameters
1 restraint
$\Delta\rho_{max}$ = 0.25 e Å$^{-3}$
$\Delta\rho_{min}$ = −0.62 e Å$^{-3}$
Absolute structure: Flack (1983), 189 Friedel pairs
Flack parameter: 0.171 (15)

**Table 1**
Selected geometric parameters (Å, °).

| | | | |
|---|---|---|---|
| Li1—O1$^{i}$ | 1.936 (10) | Mn1—O1 | 2.065 (2) |
| Li1—O3 | 1.956 (6) | Mn1—O2 | 2.090 (2) |
| Li1—O3$^{ii}$ | 1.99 (2) | Si1—O1$^{v}$ | 1.631 (3) |
| Li1—O2$^{iii}$ | 2.009 (6) | Si1—O3 | 1.6331 (17) |
| Mn1—O3$^{iv}$ | 2.0585 (16) | Si1—O2$^{vi}$ | 1.639 (2) |
| | | | |
| O1$^{i}$—Li1—O3 | 112.0 (7) | O3$^{iv}$—Mn1—O1 | 105.74 (5) |
| O1$^{i}$—Li1—O3$^{ii}$ | 107.5 (5) | O3$^{iv}$—Mn1—O2 | 107.31 (6) |
| O3—Li1—O3$^{ii}$ | 107.7 (7) | O1—Mn1—O2 | 104.54 (8) |
| O1$^{i}$—Li1—O2$^{iii}$ | 108.6 (6) | O1$^{v}$—Si1—O3 | 109.35 (10) |
| O3—Li1—O2$^{iii}$ | 113.9 (5) | O3—Si1—O3$^{vii}$ | 109.58 (13) |
| O3$^{ii}$—Li1—O2$^{iii}$ | 106.8 (6) | O1$^{v}$—Si1—O2$^{vi}$ | 108.23 (13) |
| O3$^{iv}$—Mn1—O3 | 124.58 (8) | O3—Si1—O2$^{vi}$ | 110.16 (10) |

Symmetry codes: (i) $x, y-1, z$; (ii) $-x+\frac{3}{2}, -y, z-\frac{1}{2}$; (iii) $-x+\frac{3}{2}, -y, z+\frac{1}{2}$; (iv) $-x+1, y, z$; (v) $-x+\frac{3}{2}, -y+1, z-\frac{1}{2}$; (vi) $-x+\frac{3}{2}, -y+1, z+\frac{1}{2}$; (vii) $-x+2, y, z$.

**Table 2**
Bond-valence parameters derived from the present model and the previous studies..

| Atom | Site | Present work | Dominko *et al.*[1)] | Arroyo-de Dompablo *et al.*[2)] |
|---|---|---|---|---|
| Li | 4*b* | 1.02 (6) | 1.0 (1) | 0.9 |
| Mn | 2*a* | 1.89 (5) | 2.1 (1) | 1.77 |
| Si | 2*a* | 3.89 (7) | 3.6 (2) | 3.65 |
| O1 | 2*a* | 2.02 (9) | 1.9 (3) | 1.75 |
| O2 | 4*b* | 1.97 (7) | 1.9 (2) | 1.86 |
| O3 | 2*a* | 1.87 (7) | 2.0 (2) | 1.90 |

1) The data, referred to Dominko *et al.* (2006), are based on the coordinates for primary $MO_4$ ($M$ = Li, Mn, Si) tetrahedra. 2) The data, referred to Arroyo-de Dompablo *et al.* (2008), are based on the coordinates for primary $MO_4$ ($M$ = Li, Mn, Si) tetrahedra optimized by density functional theory (DFT) methods.

Data collection: *CrystalClear* (Rigaku, 2010); cell refinement: *CrystalClear*; data reduction: *CrystalClear*; program(s) used to solve

structure: *SIR97* (Altomare *et al.*, 1999); program(s) used to refine structure: *SHELXL97* (Sheldrick, 2008); molecular graphics: *VESTA* (Momma & Izumi, 2011); software used to prepare material for publication: *WinGX* (Farrugia, 1999).

Supplementary data and figures for this paper are available from the IUCr electronic archives (Reference: WM2658).

## References


Altomare, A., Burla, M. C., Camalli, M., Cascarano, G. L., Giacovazzo, C., Guagliardi, A., Moliterni, A. G. G., Polidori, G. & Spagna, R. (1999). *J. Appl. Cryst.* **32**, 115–119.

Arroyo-de Dompablo, M. E., Armand, M., Tarascon, J. M. & Amador, U. (2006). *Electrochem. Commun.* **8**, 1292–1298.

Arroyo-de Dompablo, M. E., Dominko, R., Gallardo-Amores, J. M., Dupont, L., Mali, G., Ehrenberg, H., Jamnik, J. & Moraán, E. (2008). *Chem. Mater.* **20**, 5574–5584.

Belharouak, I., Abouimrane, A. & Amine, K. (2009). *J. Phys. Chem. C*, **113**, 20733–20737.

Brown, I. D. & Altermatt, D. (1985). *Acta Cryst.* B**41**, 244–247.

Cooper, R. I., Gould, R. O., Parsons, S. & Watkin, D. J. (2002). *J. Appl. Cryst.* **35**, 168–174.

Dominko, R., Bele, M., Gaberscek, M., Meden, A., Remskar, M. & Jamnik, J. (2006). *Electrochem. Commun.* **8**, 217–222.

Duncan, H., Kondamreddy, A., Mercier, P. H. J., Le Page, Y., Abu-Lebdeh, Y., Couillard, M., Whitfield, P. S. & Davidson, I. J. (2011). *Chem. Mater.* **23**, 5446–5456.

Farrugia, L. J. (1999). *J. Appl. Cryst.* **32**, 837–838.

Flack, H. D. (1983). *Acta Cryst.* A**39**, 876–881.

Islam, M. S., Dominko, R., Masquelier, C., Sirisopanaporn, C., Armstrong, A. R. & Bruce, P. G. (2011). *J. Mater. Chem.* **21**, 9811–9818.

Kokalj, A., Dominko, R., Mali, G., Meden, A., Gaberscek, M. & Jamnik, J. (2007). *Chem. Mater.* **19**, 3633–3640.

Kuganathan, N. & Islam, M. S. (2009). *Chem. Mater.* **21**, 5196–5202.

Mali, G., Meden, A. & Dominko, R. (2010). *Chem. Commun.* **46**, 3306–3308.

Momma, K. & Izumi, F. (2011). *J. Appl. Cryst.* **44**, 1272–1276.

Politaev, V. V., Petrenko, A. A., Nalbandyan, V. B., Medvedev, B. S. & Shvetsova, E. S. (2007). *J. Solid State Chem.* **180**, 1045–1050.

Rigaku (1998). *REQAB*. Rigaku Corporation, Tokyo, Japan.

Rigaku (2010). *CrystalClear*. Rigaku Corporation, Tokyo, Japan.

Santamaría-Pérez, D., Amador, U., Tortajada, J., Dominko, R. & Arroyo-de Dompablo, M. E. (2012). *Inorg. Chem.* **51**, 5779–5786.

Setoguchi, M. (1988). *Osaka Kogyo Gijutsu Shikensho Hokoku*, pp. 1–83.

Sheldrick, G. M. (2008). *Acta Cryst.* A**64**, 112–122.

Sirisopanaporn, C., Dominko, R., Masquelier, C., Armstrong, A. R., Mali, G. & Bruce, P. G. (2011). *J. Mater. Chem.* **21**, 17823–17831.

West, A. R. & Glasser, F. P. (1972). *J. Solid State Chem.* **4**, 20–28.

Wu, S. Q., Zhu, Z. Z., Yang, Y. & Hou, Z. F. (2009). *Comput. Mater. Sci.* **44**, 1243–1251.

Yamaguchi, H., Akatsuka, K., Setoguchi, M. & Takaki, Y. (1979). *Acta Cryst.* B**35**, 2680–2682.

Zhong, G., Li, Y., Yan, P., Liu, Z., Xie, M. & Lin, H. (2010). *J. Phys. Chem.* C**114**, 3693–3700.

# supplementary materials

*Acta Cryst.* (2012). E**68**, i68–i69 [doi:10.1107/S1600536812035040]

## Redetermination of the low-temperature polymorph of $Li_2MnSiO_4$ from single-crystal X-ray data

**Mineo Sato, Tadashi Ishigaki, Kazuyoshi Uematsu, Kenji Toda and Hirokazu Okawa**

### Comment

Lithium transition metal orthosilicates $Li_2MSiO_4$ ($M$ = Mn, Fe, Co) have recently become attracting and received much attention as alternatives for the currently used cathode materials of lithium ion batteries, such as $LiCoO_2$, $Li(Ni,Mn,Co)O_2$, $LiMn_2O_4$ and $LiMPO_4$ ($M$ = Fe, Mn), because of the natural abundance of silica, iron, and manganese, but also due to a possible high theoretical capacity through two electron delivery. In order to understand the intercalation mechanism of $Li^+$ ions in $Li_2MSiO_4$ cathode materials, their crystal structures have been investigated mainly by means of powder methods using X-ray or synchrotron radiation. Summarized by structural studies up-to-date (Islam *et al.*, 2011; Santamaría-Pérez *et al.*, 2012), it could be concluded that the $Li_2MSiO_4$ compounds ($M$ = Fe, Mn, Co) belong to a large family of materials known as derivatives of $Li_3PO_4$, where oxygen atoms form arrays with a distorted hexagonal-close-packing (*hcp*) within which half of the tetrahedral voids are occupied by cations. Depending on which site (up or down) of the array the cations occupy, the material shows a rich polymorphism. Such compounds may be divided into two families, designated as $\beta$- and $\gamma$-forms after the notations used for $Li_3PO_4$ polymorphs (West & Glasser, 1972). The $\gamma$-polymorphs are built up of both corner- and edge-sharing tetrahedra with half of the tetrahedra pointing along one direction perpendicular to the *hcp* array and the other half pointing along the opposite direction, while the $\beta$-polymorphs are built up of only corner-sharing tetrahedra, with all the tetrahedra pointing to the same direction perpendicular to the *hcp* array. Detailed structural information, particularly for electrochemically active $Li_2MnSiO_4$, were available from the previous studies. $Li_2MnSiO_4$ exhibit three polymorphs, namely a low-temperature form denoted as $\beta_{II}$ ($Pmn2_1$), an intermediate temperature form denoted as $\gamma_{II}$ ($Pmnb$), and a high-temperature form denoted as $\gamma_o$ ($P2_1/n$) (Arroyo-de Dompablo *et al.*, 2006, 2008; Belharouak *et al.*, 2009; Dominko *et al.*, 2006; Kokalj *et al.*, 2007; Politaev *et al.*, 2007; Wu *et al.*, 2009; Zhong *et al.*, 2010). It should be noted that in almost all polymorphs a site disorder for cationic sites, particularly for $Li^+$ sites substituted by transition metal ions, was observed. Surprisingly, the structure models proposed for $Li_2MSiO_4$ ($M$ = Mn, Fe, Co) have all been determined and refined by powder diffraction methods except for that of $Li_2CoSiO_4$ (Yamaguchi *et al.*, 1979). In terms of the fact that lithium has quite low scattering factors for X-rays, this may be true even for neutron diffraction, the crystallographic information obtained for Li sites by powder diffraction should inevitably include ambiguity to some extent. Efforts to obtain single crystals for structure determination have not been rewarded for $Li_2MSiO_4$ ($M$ = Mn, Fe). Although Setoguchi (1988) succeeded to grow single crystals of $Li_2FeSiO_4$ from a flux method using LiCl at elevated temperatures, he could not determine the structure because of suffering from twinned crystals. Here we describe the single-crystal growth of $Li_2MnSiO_4$ by means of a high temperature hydrothermal method and its structure determination using single-crystal X-ray diffraction, confirming a perfectly site-ordered structure for $Li_2MnSiO_4$ in its low-temperature $\beta_{II}$ ($Pmn2_1$) polymorph.

The first detailed report on the description of the structure model for $Li_2MnSiO_4$ accompanied with numerical crystallographic data is probably that determined by Dominko *et al.* (2006) who performed Rietveld refinements in the space group $Pmn2_1$ with $a$ = 6.3109 (9) Å, $b$ = 5.3800 (9) Å, $c$ = 4.9662 (8) Å and $Z$ = 2. The obtained structure model is presented in Fig. 1. It contains significant site disorders for all cationic sites, though the primary sites for the cations are located within the tetrahedral voids situated among a fairly distorted hexagonal-close-packing (*hcp*) of oxygen atoms. The $MO_4$ ($M$ = Li, Mn, Si) tetrahedra all point towards the same direction perpendicular to the *hcp* array, and are linked by corner-sharing. The partially occupied tetrahedral sites are located on the opposite sides of corresponding primary $MO_4$ tetrahedra, the vertices of which point to the opposite direction. The central metal atom pairs are separated by distances of 1.0 (2) Å for Li—Li pairs, 0.52 (10) Å for Mn—Mn pairs and 1.09 (15) Å for Si—Si pairs, forming kinds of (pseudo) trigonal-bipyramidal $MO_5$ polyhedra, as shown in Fig. 1(*b*). The structure can also be described as a typical $\beta_{II}$-$Li_3PO_4$ structure if cation sites with low site-occupancies are removed, as shown in Fig. 1(*c*) and (*d*). This structure model, which has such excessive disorders, may have somewhat possible deficiencies. Furthermore, the environment around $Li^+$ ions is crucially important for understanding the lithium intercalation behavior during the charge/discharge process. Theroretical studies concerned with expectation of redox potentials and lithium migration paths for $Li_2MnSiO_4$ cathodes have been accomplished by several groups (Kokalj *et al.* 2007; Kuganathan & Islam, 2009; Wu *et al.* 2009; Mali *et al.* 2010; Zhong *et al.* 2010; Duncan *et al.* 2011) based on the model by Dominko *et al.* (2006); most of these studies adopted the cation site disorder model or the idealized ordered one only with primary sites.

The structure refined in the present study is a perfectly site-ordered one for all cationic sites (Fig. 2) though the fundamental framework structure is the same as that previously reported. Notably, the displacement ellipsoids are relatively large not only for lithium atoms but also for manganese atoms (Fig. 3). This may reflect a high diffusibility both of $Li^+$ and $Mn^{2+}$ ions in this cathode material. The ordered structure model found in the present study is consistent with the results of an NMR study by Sirisopanaporn *et al.* (2011). Unexpectedly, information on atomic coordinates available for $Li_2MnSiO_4$ is scarce in the literature, where the data were refined from powder diffraction analyses (Dominko *et al.*, 2006) and obtained from an optimization by atomistic simulation (Arroyo-de Dompablo *et al.*, 2008). Table 2 shows the results of the bond-valence sum (BVS) analysis (Brown & Altermatt, 1985) for cation tetrahedra estimated from refined atomic coordinates in $Li_2MnSiO_4$, together with those for the structure models proposed previously for comparison. The deviations from the formal valences of each ion are fairly large for the previous studies, in particularly for Si, while in the present study the values of the BVS calculation for all ions are in very good agreement with the theoretical ones. Moreover, it should be mentioned that the $MO_4$ tetrahedra in the present model have much more regular environments than the previous models.

No structural data based on single-crystal X-ray diffraction data have been reported for $Li_2MnSiO_4$, although recent works on positive electrode materials for rechargeable lithium batteries reported the electrochemical characterization of this cathode material. Our present structural study of $Li_2MnSiO_4$ provides more accurate information of its crystal structure than has been available up to now.

## Experimental

In order to synthesize $Li_2MnSiO_4$ single crystals, a high-temperature, high-pressure hydrothermal synthetic method was performed in a silver ampoule contained in a home-made autoclave made of stainless steel (SUS304) with 6 cm in outer diameter, 0.8 cm in inner diameter, and 1.8 $cm^3$ in volume. The pressure was provided by water. High-purity chemical reagents of $MnO_2$, $SiO_2$ and $LiOH{\cdot}2H_2O$ were used as reaction agents. A reaction mixture of LiOH, $MnO_2$ and $SiO_2$ with a molar ratio of Li:Mn:Si = 2:12:2 in a 3 cm long silver ampoule (inside diameter = 0.6 cm) was heated at 823 K for 3 days. The pressure was estimated to be 12 MPa at the reaction temperature according to the pressure-temperature

diagram of pure water. The autoclave was then cooled to 323 K at 5 K/h and quenched to room temperature by removing the autoclave from the furnace. The product was filtered off, washed with water, rinsed with ethanol, and dried at ambient temperature. The reaction produced light-green rod-shaped crystals of $Li_2MnSiO_4$ that were obtained as a major product along with some quartz crystals.

The surface of the single crystals was observed by using optical (Olympus BX-60) and scanning electron microscopy (SEM, Jeol JSM-5310LVB). The elemental composition of the crystals was characterized by energy dispersive X-ray spectroscopy (EDS) attached to SEM (SEM/EDS, Nippon Denshi JED-2140).

## Refinement

The structure was solved by direct methods and refined by subsequent Fourier syntheses, leading to $wR2 = 4.17\%$ in the early stages of refinement. The relatively high value of the Flack parameter, $x = 0.167$, pointed to a possible twinned crystal. The examination using *ROTAX* (Cooper *et al.*, 2002) indicated two possible rotation twin axes about [010] and [001]. In addition to these rotation twin formations, a racemic twin (inversion twin) formation can be also possible for the non-centrosymmetric $Pmn2_1$ space group. Subsequent refinements using the twin laws for the three cases yielded a satisfactory solution with $wR2 = 3.67\%$ for all cases and a Flack parameter $x = 0.00$ (2) for the rotation twin cases. The twin fraction ratio is 82.9: 17.1. In non-centrosymmetric space groups where mirror planes and/or glide planes exist, an inversion twin is equivalent to the rotation twin through the 2-fold rotation axis perpendicular to the mirror and/or the glide planes. This is true for the present case.

## Computing details

Data collection: *CrystalClear* (Rigaku, 2010); cell refinement: *CrystalClear* (Rigaku, 2010); data reduction: *CrystalClear* (Rigaku, 2010); program(s) used to solve structure: *SIR97* (Altomare *et al.*, 1999); program(s) used to refine structure: *SHELXL97* (Sheldrick, 2008); molecular graphics: *VESTA* (Momma & Izumi, 2011); software used to prepare material for publication: *WinGX* (Farrugia, 1999).

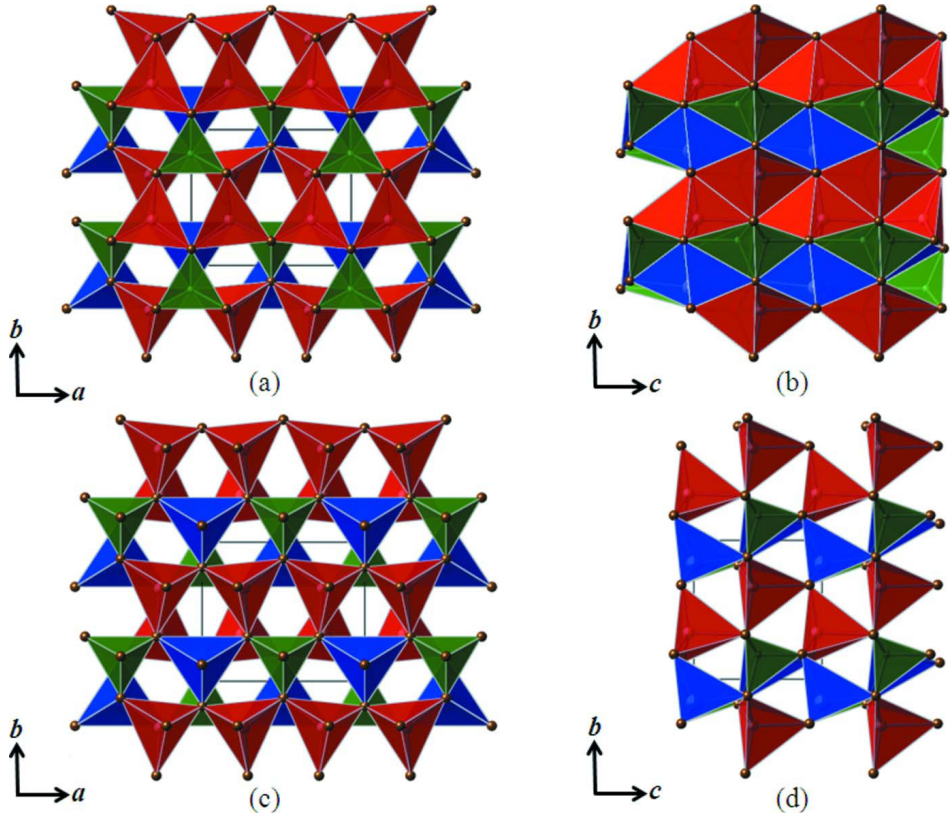


**Figure 1**

Structure model of $Li_2MnSiO_4$ determined by Dominko *et al.* (2006). The original structure model is projected (*a*) along [001] and (*b*) along [100], while the structure model where cation sites with low occupancies are removed is projected (*c*) along [001] and (*d*) along [100]. Polyhedra are indicated by red color for $LiO_4$, blue color for $MnO_4$, and green color for $SiO_4$.

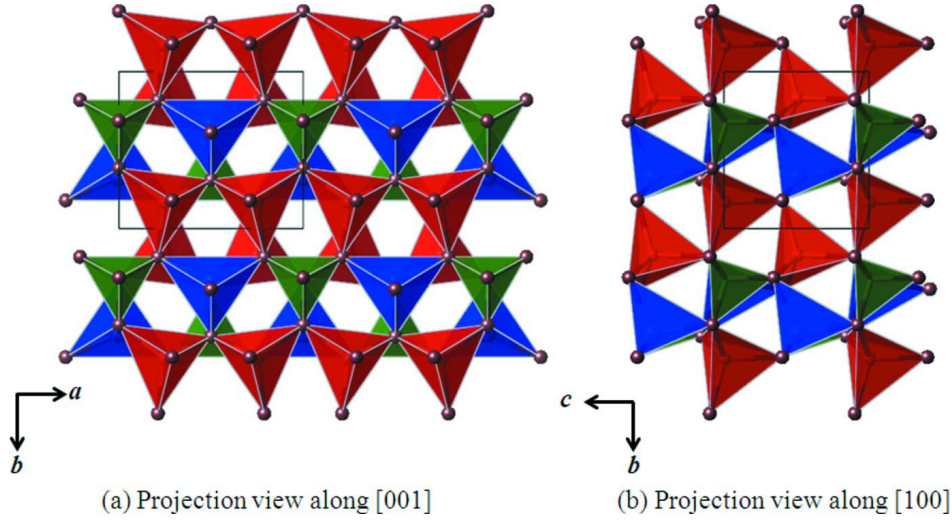


**Figure 2**

Structure model of $Li_2MnSiO_4$ determined by the present study with (*a*) projection view along [001] and (*b*) projection view along [100]. Polyhedra are indicated by red color for $LiO_4$, blue color for $MnO_4$, and green color for $SiO_4$.

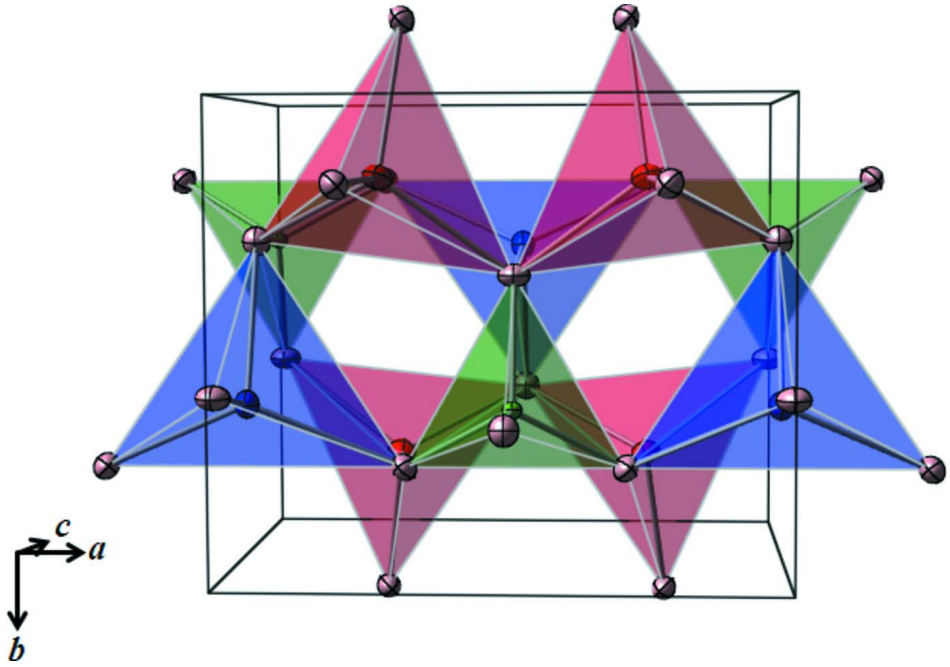


**Figure 3**

A perspective view of a part of the $Li_2MnSiO_4$ structure with the unit cell outlined. Displacement ellipsoids are drawn at the 70% probability level. Polyhedra are indicated by red color for $LiO_4$, blue color for $MnO_4$, and green color for $SiO_4$.

**dilithium manganese(II) silicate**

*Crystal data*

$Li_2MnSiO_4$
$M_r$ = 160.91
Orthorhombic, $Pmn2_1$
Hall symbol: P 2ac -2
$a$ = 6.3133 (16) Å
$b$ = 5.3677 (14) Å
$c$ = 4.9685 (12) Å
$V$ = 168.37 (7) Å$^3$
$Z$ = 2
$F(000)$ = 154
$D_x$ = 3.174 Mg m$^{-3}$
Mo $K\alpha$ radiation, $\lambda$ = 0.71069 Å
Cell parameters from 1684 reflections
$\theta$ = 3.2–27.5°
$\mu$ = 4.11 mm$^{-1}$
$T$ = 295 K
Prism, light green
0.26 × 0.19 × 0.18 mm

*Data collection*

Rigaku Mercury375R diffractometer
Radiation source: Sealed Tube
Graphite monochromator
Detector resolution: 13.6612 pixels mm$^{-1}$
profile data from $\omega$–scans
Absorption correction: multi-scan (*REQAB*; Rigaku, 1998)
$T_{min}$ = 0.377, $T_{max}$ = 0.477
1636 measured reflections
423 independent reflections
419 reflections with $I > 2\sigma(I)$
$R_{int}$ = 0.019
$\theta_{max}$ = 27.4°, $\theta_{min}$ = 3.8°
$h$ = −8→8
$k$ = −6→6
$l$ = −6→6

*Refinement*

Refinement on $F^2$
Least-squares matrix: full
$R[F^2 > 2\sigma(F^2)] = 0.015$
$wR(F^2) = 0.037$
$S = 1.14$
423 reflections
45 parameters
1 restraint
0 constraints
Primary atom site location: structure-invariant direct methods
Secondary atom site location: difference Fourier map
$w = 1/[\sigma^2(F_o^2) + (0.0217P)^2]$ where $P = (F_o^2 + 2F_c^2)/3$
$(\Delta/\sigma)_{max} < 0.001$
$\Delta\rho_{max} = 0.25$ e Å$^{-3}$
$\Delta\rho_{min} = -0.62$ e Å$^{-3}$
Extinction correction: *SHELXL97* (Sheldrick, 2008), $Fc^* = kFc[1+0.001xFc^2\lambda^3/\sin(2\theta)]^{-1/4}$
Extinction coefficient: 0.392 (13)
Absolute structure: Flack (1983), 189 Friedel pairs
Flack parameter: 0.171 (15)

*Special details*

**Geometry**. All s.u.'s (except the s.u. in the dihedral angle between two l.s. planes) are estimated using the full covariance matrix. The cell s.u.'s are taken into account individually in the estimation of s.u.'s in distances, angles and torsion angles; correlations between s.u.'s in cell parameters are only used when they are defined by crystal symmetry. An approximate (isotropic) treatment of cell s.u.'s is used for estimating s.u.'s involving l.s. planes.

**Refinement**. Refinement of $F^2$ against ALL reflections. The weighted *R*-factor *wR* and goodness of fit *S* are based on $F^2$, conventional *R*-factors *R* are based on *F*, with *F* set to zero for negative $F^2$. The threshold expression of $F^2 > 2\sigma(F^2)$ is used only for calculating *R*-factors(gt) *etc*. and is not relevant to the choice of reflections for refinement. *R*-factors based on $F^2$ are statistically about twice as large as those based on *F*, and *R*- factors based on ALL data will be even larger.

*Fractional atomic coordinates and isotropic or equivalent isotropic displacement parameters (Å²)*

| | *x* | *y* | *z* | $U_{iso}$*/$U_{eq}$ |
|---|---|---|---|---|
| Li1 | 0.7503 (4) | −0.1688 (4) | 0.995 (5) | 0.0090 (7) |
| Mn1 | 0.5 | 0.33172 (5) | 0.9968 | 0.00733 (15) |
| Si1 | 1 | 0.32090 (9) | 0.9851 (3) | 0.00350 (17) |
| O1 | 0.5 | 0.6868 (3) | 1.1569 (5) | 0.0071 (5) |
| O2 | 0.5 | 0.3867 (3) | 0.5804 (4) | 0.0081 (4) |
| O3 | 0.7887 (2) | 0.1799 (2) | 1.0979 (4) | 0.0075 (3) |

*Atomic displacement parameters (Å²)*

| | $U^{11}$ | $U^{22}$ | $U^{33}$ | $U^{12}$ | $U^{13}$ | $U^{23}$ |
|---|---|---|---|---|---|---|
| Li1 | 0.0084 (17) | 0.0061 (15) | 0.0125 (15) | −0.0009 (7) | 0.0000 (14) | −0.002 (2) |
| Mn1 | 0.0055 (2) | 0.0072 (2) | 0.0093 (2) | 0 | 0 | 0.0000 (2) |
| Si1 | 0.0035 (3) | 0.0028 (3) | 0.0042 (4) | 0 | 0 | −0.0003 (3) |
| O1 | 0.0075 (9) | 0.0083 (8) | 0.0056 (11) | 0 | 0 | −0.0004 (6) |
| O2 | 0.0098 (8) | 0.0048 (7) | 0.0096 (10) | 0 | 0 | 0.0001 (7) |
| O3 | 0.0068 (5) | 0.0067 (6) | 0.0089 (7) | −0.0009 (4) | 0.0008 (7) | 0.0000 (5) |

*Geometric parameters (Å, º)*

| | | | |
|---|---|---|---|
| Li1—O1$^{i}$ | 1.936 (10) | Mn1—O1 | 2.065 (2) |
| Li1—O3 | 1.956 (6) | Mn1—O2 | 2.090 (2) |
| Li1—O3$^{ii}$ | 1.99 (2) | Si1—O1$^{v}$ | 1.631 (3) |
| Li1—O2$^{iii}$ | 2.009 (6) | Si1—O3 | 1.6331 (17) |
| Mn1—O3$^{iv}$ | 2.0585 (16) | Si1—O3$^{vi}$ | 1.6331 (17) |

| | | | |
|---|---|---|---|
| Mn1—O3 | 2.0585 (15) | Si1—O2$^{vii}$ | 1.639 (2) |
| | | | |
| O1$^{i}$—Li1—O3 | 112.0 (7) | O3$^{iv}$—Mn1—O2 | 107.31 (6) |
| O1$^{i}$—Li1—O3$^{ii}$ | 107.5 (5) | O3—Mn1—O2 | 107.31 (6) |
| O3—Li1—O3$^{ii}$ | 107.7 (7) | O1—Mn1—O2 | 104.54 (8) |
| O1$^{i}$—Li1—O2$^{iii}$ | 108.6 (6) | O1$^{v}$—Si1—O3 | 109.35 (10) |
| O3—Li1—O2$^{iii}$ | 113.9 (5) | O1$^{v}$—Si1—O3$^{vi}$ | 109.35 (10) |
| O3$^{ii}$—Li1—O2$^{iii}$ | 106.8 (6) | O3—Si1—O3$^{vi}$ | 109.58 (13) |
| O3$^{iv}$—Mn1—O3 | 124.58 (8) | O1$^{v}$—Si1—O2$^{vii}$ | 108.23 (13) |
| O3$^{iv}$—Mn1—O1 | 105.74 (5) | O3—Si1—O2$^{vii}$ | 110.16 (10) |
| O3—Mn1—O1 | 105.74 (5) | O3$^{vi}$—Si1—O2$^{vii}$ | 110.16 (10) |

Symmetry codes: (i) $x$, $y$−1, $z$; (ii) −$x$+3/2, −$y$, $z$−1/2; (iii) −$x$+3/2, −$y$, $z$+1/2; (iv) −$x$+1, $y$, $z$; (v) −$x$+3/2, −$y$+1, $z$−1/2; (vi) −$x$+2, $y$, $z$; (vii) −$x$+3/2, −$y$+1, $z$+1/2.

*Bond-valence parameters derived from the present model and the previous studies.*

| Atom | Site | Present work | Dominko *et al.*[1)] | Arroyo-de Dompablo *et al.*[2)] |
|---|---|---|---|---|
| Li | 4*b* | 1.02 (6) | 1.0 (1) | 0.9 |
| Mn | 2*a* | 1.89 (5) | 2.1 (1) | 1.77 |
| Si | 2*a* | 3.89 (7) | 3.6 (2) | 3.65 |
| O1 | 2*a* | 2.02 (9) | 1.9 (3) | 1.75 |
| O2 | 4*b* | 1.97 (7) | 1.9 (2) | 1.86 |
| O3 | 2*a* | 1.87 (7) | 2.0 (2) | 1.90 |

1) The data, referred to Dominko *et al.* (2006), are based on the coordinates for primary $MO_4$ ($M$ = Li, Mn, Si) tetrahedra. 2) The data, referred to Arroyo-de Dompablo *et al.* (2008), are based on the coordinates for primary $MO_4$ ($M$ = Li, Mn, Si) tetrahedra optimized by density functional theory (DFT) methods.